

Propagation of the photoelectron wave packet in an attosecond streaking experiment

E. E. Krasovskii,^{1,2,3} C. Friedrich,⁴ W. Schattke,^{5,2} and P. M. Echenique^{1,2,6}

¹*Departamento de Física de Materiales, Facultad de Ciencias Químicas, Universidad del País Vasco/Euskal Herriko Unibertsitatea, San Sebastián/Donostia, Spain*

²*Donostia International Physics Center (DIPC), San Sebastián/Donostia, Spain*

³*IKERBASQUE, Basque Foundation for Science, Bilbao, Spain*

⁴*Peter Grünberg Institute and Institute for Advanced Simulation, Forschungszentrum Jülich and JARA, 52425 Jülich, Germany*

⁵*Institut für Theoretische Physik und Astrophysik der Christian-Albrechts-Universität zu Kiel, Leibnizstraße 15, 24118 Kiel*

⁶*Centro de Física de Materiales CFM - Materials Physics Center MPC, Centro Mixto CSIC-UPV/EHU, Edificio Korta, Avenida de Tolosa 72, 20018 San Sebastián, Spain*

Laser-assisted photoemission from a solid is considered within a numerically exactly solvable one-dimensional model of a crystal. The effect of the inelastic scattering and of the finite duration of the pump pulse on the photoelectron dynamics is elucidated. The phenomenological result that the photoexcited wave packet moves with the group velocity dE/dk and traverses on average the distance equal to the mean free path is found to hold for energies far from the spectral gaps of the final state band structure. On the contrary, close to a spectral gap the photoelectron is found to move during the excitation by the pump pulse with a velocity higher than the group velocity.

INTRODUCTION

Transport properties of electron wave packets underlie the functioning of electronic devices and are an important factor in photoemission spectroscopies and electron diffraction techniques. In a solid, as opposed to a single atom, special role is played by inelastic scattering giving rise to a limited electron lifetime and mean free path. The inelastic scattering is phenomenologically described as electron absorption [1], and its implications for stationary processes are well understood [2–7]. A much less studied question is how the wave packet evolves and propagates on a time scale comparable to its lifetime. Experimental access to such ultrafast processes is given by modern time-resolved photoelectron spectroscopies, in particular by the streaking method [8–12], in which a subfemtosecond time resolution is achieved by mapping time to energy using a strong laser field: the electron wave packet created by an ultrashort pulse of extreme ultraviolet radiation (XUV) is accelerated by the superimposed laser field, and the energy by which its spectrum shifts up or down depends on the electron release time t_x relative to the temporal profile of the laser field $E_L(t)$.

Various models have been developed that treated the problem by the time-dependent Schrödinger equation (TDSE) [13–16] or by applying a classical model [17]. The majority of the studies consider a solid in which the low-frequency laser field is strongly damped by the dielectric response [18], so the electron needs to travel some distance before it gets exposed to the streaking field.

MEAN FREE PATH OR LIFETIME?

Assuming an instantaneous XUV excitation, the time of flight from the depth where the photoelectron is cre-

ated to the surface is determined by the group velocity of the wave packet. Because of the inelastic scattering the photoelectrons excited deeper in the crystal have smaller probability to reach the detector, which is assumed to scale with the depth z as $\exp(z/\lambda)$. Then the average depth traversed by the electrons is just the mean free path (MFP) λ , and the time to reach the surface can be estimated as $\tau = \lambda/v$, where v is the group velocity of the emitted wave packet [12]. Often it is sufficient to use the values of λ averaged over an energy interval of several eVs that can be inferred from the well-known universal

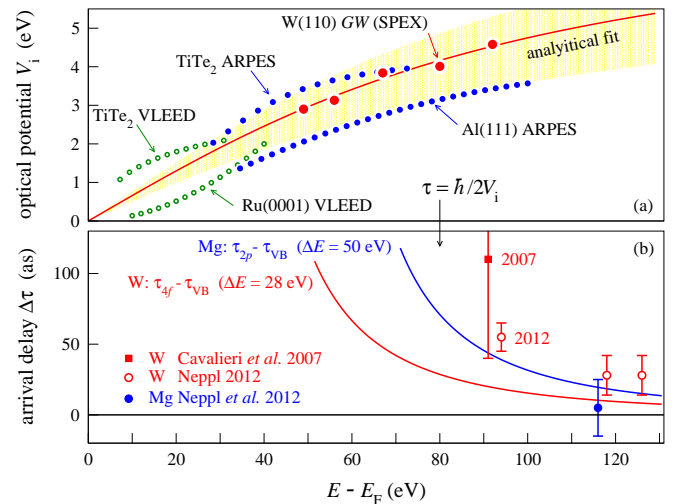


FIG. 1: Dependence of optical potential V_i on energy. Small circles are the values empirically derived from *ab initio* analysis of ARPES spectra (full circles) and VLEED spectra (open circles). Large circles are the *ab initio* GW calculation for W(100) (FLEUR-SPEX). The dependence $V_i(E)$ is well fitted by a function $\gamma \arctan(E/\beta)$ with $\beta = 80$ eV and $\gamma = 5.3$ eV for W(100), $\gamma = 4$ eV for Al(111), and $\gamma = 6.2$ eV for TiTe₂.

$\lambda(E)$ curve. This is, however, not sufficient for ARPES because MFP may strongly vary over a few eV interval as a result of the specific band structure. At the same time, experience with ARPES and VLEED (very low energy electron diffraction) [3–7] suggests that the photoelectron final-state lifetime changes rather smoothly with energy, see Fig. 1(a). Thus, it is reasonable to rely on the average values for the lifetime, and to derive the rapidly varying MFP as $\lambda = vt = v/V_i$, where V_i is the inverse lifetime (optical potential), which enters the Hamiltonian through the imaginary term $-iV_i$. For a nearly free electron, the wave vector k acquires an imaginary part $\kappa = mV_i/\hbar^2$, which yields $\lambda = 1/2\kappa$, and the time to reach the surface is then

$$\tau = \frac{\hbar}{2V_i}. \quad (1)$$

Note that the group velocity cancels, so τ depends on energy through the function $V_i(E)$. Vast empirical data suggest that the $V_i(E)$ curves are similar for different materials: V_i grows with energy with similar rate, see Fig. 1(a). Because the empirically derived data may be affected by various extrinsic factors and by the imperfection of the apparatus it is important to theoretically corroborate this observation. Microscopically, optical potential is associated with the imaginary part of the self-energy. Figure 1(a) shows an *ab initio* *GW* calculation for a high-energy conducting band of W(110). It is seen to agree well with the empirical results, which supports our understanding of the electron absorption as coming predominantly from the electron-electron interaction and corroborates the empirical estimate of its growth with energy.

Thus, within this simplest approach the arrival delay of photoelectrons with final energy E relative to those with energy $E + \epsilon$ behaves roughly as $\Delta\tau(E) \sim \epsilon/E(E - \epsilon)$, see Fig. 1(b): the electron with a lower energy comes later, and the delay $\Delta\tau$ decreases as the final state energy grows. The recent measurements by Neppl [19] on W(110) of the phase shift between the spectrograms of valence $5d$ and semi-core $4f$ states qualitatively follow this trend [open circles in Fig. 1(b)], but the absolute values in the experiment are about three times larger. At the same time, the value of 5 ± 20 as measured on Mg(0001) at $\hbar\omega = 118$ eV is 4 times smaller than expected from the simple MFP-based theory.

FUNDAMENTAL QUESTIONS

Such drastic disagreement in absolute values calls for the search of mechanisms that, in addition to the finite lifetime, affect the transport of the photoelectron to the surface. A number of fundamental questions arise: What is the role of the finite duration of the pump pulse, i.e., at what point does the wave packet start its motion with the

group velocity? Does the electron have the group velocity dictated by the band structure if it travels only the distance of a few atomic layers? How does the packet propagate when its energy falls into a forbidden gap, where the group velocity cannot be defined as dE/dk ? Can the electron excited at the outermost atomic plane be thought of as not feeling the band structure because it moves away from the surface, towards vacuum?

Apart from that, an important theoretical question arises of whether the absorbing potential $-iV_i$ can be used in the time-dependent Schrödinger equation to adequately describe both the photocurrent attenuation and the implications for the transport: inelastic scattering is a stochastic process, so the photocurrent is an incoherent overlap of randomly dephased contributions, whereas the optical-potential-damped wave packet remains fully coherent, which may have implications both for its transport and for its acceleration by the laser field.

THE MODEL

To resolve these questions, we need a model that does not incorporate any assumptions about the answers and, at the same time, can be treated numerically exactly. For the present proof-of-concept calculation we use a one-dimensional model of a crystal, which treats photoexcitation, transport, and streaking fully quantum-mechanically without resorting to a perturbational treatment of any of the terms in the Hamiltonian or to a heuristic separation of the XUV and the laser pulses. We employ a particle-in-the-box method: the box comprises a thick crystal slab lying on a structureless substrate [the piecewise constant potential $V(z)$ in Fig. 2(a)] and the vacuum half-space. In Ref. [20] this model was applied to photoelectron streaking by a spatially uniform laser field in the absence of inelastic scattering. The present model allows for a rapid decay of the laser field into the solid and includes the inelastic scattering in two alternative ways: via the optical potential and by a straightforward ensemble averaging over random configurations.

THE PROCEDURE

We perform a series of numerical experiments, in which the system is excited by an XUV pulse of duration $D_x = 1$ fs and is simultaneously acted upon by the laser pulse of duration $D_L = 5$ fs, Fig. 2(b). Both light fields are given by the dipole operator z , and the laser field is screened by a multipolar l by a smooth step function $\theta(z)$. The temporal envelopes of both pulses are of the form $\cos^2(\pi t/D)$. The laser pulse is $\mathcal{E}_L(t) = \mathcal{E}_L^M \sin \Omega(t - t_L) \cos^2[\pi(t - t_L)/D_L]$, with photon energy $\Omega = 1.65$ eV and amplitude $\mathcal{E}_L^M = 2 \times 10^7$ V/cm. The TDSE is solved with the split-operator technique in ma-

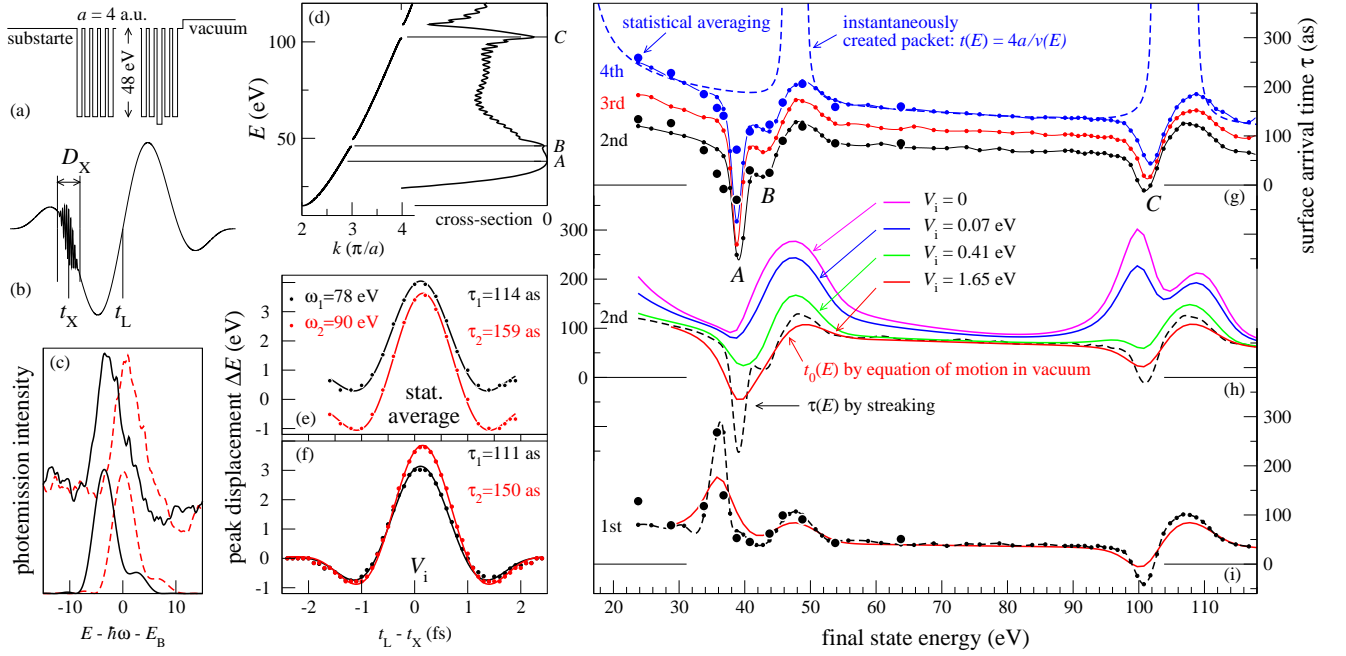


FIG. 2: (a) Crystal potential $V(z)$ with a defect at the third layer. (b) Superposition of the XUV and the laser pulses. (c) Streaked spectra for $\hbar\omega = 78$ eV with absorption (lower curves) and with random collisions (upper curves) for $t_L - t_X = 1600$ as (solid lines) and 200 as (dashed lines). (d) Band structure with the periodic potential $V(z)$ and energy dependence of the cross-section of emission from a localized state at a defect. (e) and (f) Streaking curves for $\hbar\omega = 78$ and 90 eV with random collisions (e) and with an absorption (f). (g)–(i) Surface arrival time as function of the final state energy. Small circles connected by solid lines in graph (g) and dashed lines in (h) and (i) are streaking results with absorption. Large circles in graphs (g) and (i) are streaking with random collisions. Solid lines in graphs (h) and (i) are from the equation of motion in vacuum.

trix form in terms of exact eigenfunctions (discrete spectrum) of the unperturbed Hamiltonian $\hat{H} = \hat{p}^2/2m + V$, so the crystal potential is fully taken into account for both initial and final states. The spectrum of \hat{H} is truncated at 200 eV above the vacuum level, which ensures the convergence of all the results [22].

Apart from \hat{H}_0 and the two external fields the Hamiltonian includes inelastic scattering, which is either a static absorbing potential $-iV_i[1 - \theta(z)]$ or a stochastic perturbation $q(t)s_n(z)[1 - \theta(z)]$, where $q(t)$ and $s_n(z)$ are random functions of t and z , respectively. Here $q(t)$ is fixed and s_n is the n th sample in a random ensemble. The ultimate spectrum is then the average over N_R random walks, Fig. 2(c). The peak displacement ΔE from its laser-free position as a function of the time shift $\Delta t = t_L - t_X$ between the XUV and the laser pulse gives the key to the temporal information [23]: by fitting the measured $\Delta E(\Delta t)$ points with the momentum transfer function $p(\tau) = e \int_{\tau}^{\infty} dt \mathcal{E}_L(t - t_X)$, we infer the arrival time of the electron in vacuum τ , see Fig. 2(e) for the motion in the random potential and Fig. 2(f) for the motion in the absorbing potential.

RESULT: XUV PULSE SHIFTS PACKET

For a detailed study of the photoelectron transport to the surface it is convenient to exactly know its initial position in space. This is achieved by introducing a small defect at one of the layers and considering the photoemission from the localized state at the defect.

Figures 2(e) and 2(f) show streaking curves for the initial state localized at the third layer for $\hbar\omega = 78$ and 90 eV. Note that the results by the phenomenological absorbing potential (f) and by the microscopic random collisions (e) perfectly agree. Counterintuitively, the electron at the higher energy arrives 40 as later than at the lower energy: $\tau = 150$ as at 90 eV and $\tau = 111$ as at 78 eV. Figure 2(g) shows the arrival time of the electron initially at the 2nd, 3rd, and 4th layer for photon energies from 65 to 159 eV. The most striking are the two minima at $\hbar\omega = 80$ and at 143 eV ($E = 39$ and at 102 eV), at which the arrival time even shows negative values.

The minima B and C are located at the lower edges of the band gaps, and minimum A occurs at the energy where the ionization cross-section vanishes, see Fig. 2(d). There the $\tau(E)$ curve strongly deviates from that derived from the group velocity, $t(E) = d/v(E)$ [dashed curve in Fig. 2(g)]. To prove that the discrepancy is not due to the rather indirect streaking method to measure τ , we

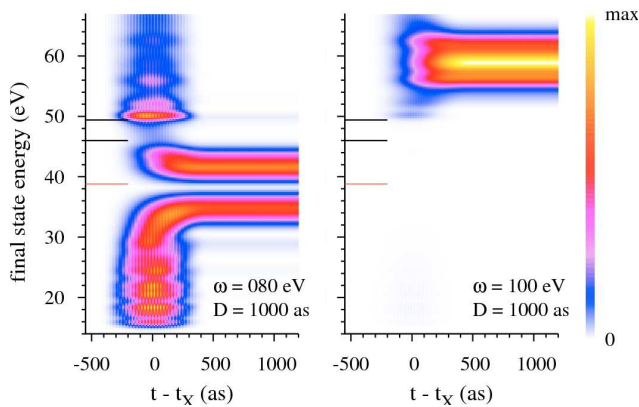


FIG. 3: Temporal evolution of the photoelectron spectrum from a localized state at $\hbar\omega = 80$ eV (left) and $\hbar\omega = 100$ eV (right). The black bars at 46 and 50 eV indicate a spectral gap, and the red bar at 39 eV indicates the Cooper minimum.

employ an alternative method: we switch off the laser and follow the propagation of the wave packet up to a distance of 500 a.u. away from the surface. By measuring the center of gravity of the packet in a number of time points we determine its equation of motion in vacuum $z_0 + \tilde{v}t$ and obtain the time point t_0 at which it has arrived at the surface. The $t_0(E)$ and $\tau(E)$ curves are seen to agree well, Fig. 2(h), which means that the clock provided by the streaking technique is accurate, and that the fast delivery of the photoelectron to the surface is effected during the excitation process. Figure 3 shows the time evolution of the spectrum at the $\tau(E)$ minimum, $\hbar\omega = 80$ eV, and at $\hbar\omega = 100$ eV, where $\tau(E)$ well agrees with the instantaneous approximation $d/v(E)$. The spectral evolution maps in the two cases are qualitatively different: while at 100 eV the spectrum rapidly concentrates around $E = \hbar\omega + E_i$, at 80 eV the evolution is much slower: at $t = 200$ as the intensity is still spread over a 40 eV wide spectral interval. Clearly, while the spectral coefficients $\psi(E, t)$ of the packet $\int dE \psi(E, t) | E \rangle$ keep changing, the velocity of its gravity center may deviate from the weighted group velocity of the stationary waves $| E \rangle$, and during the XUV pulse the wave packet may travel a distance comparable with the mean free path.

Such unusual behavior happens every time when the central energy of the wave packet approaches an intensity minimum, be it a vanishing matrix element (Cooper minimum) or a spectral gap. For the emission from the first layer, at its Cooper minimum ($\hbar\omega = 77$ eV) the XUV pulse, on the contrary, detains the packet in the solid causing a delay of ~ 200 as. All the other features of the $\tau(E)$ curve are similar to those of the emission from the deeper layers.

Figure 2(h) shows that the inelastic scattering plays an important role in the formation of the spatial shape and transport of the packet: the displacement effect is more pronounced at larger V_i . In this phenomenological

approach the dephasing of the wave packet is neglected, and the question arises if this may bring about any artifacts. This simplification turns out to be not crucial: Figure 2(g) shows the $\tau(E)$ data by statistical averaging over 144 configurations (large circles) for emission from the 2nd and 4th layer and Fig. 2(i) for the 1st layer. The parameters of the random perturbation are chosen such that it gives the same MFP as $V_i = 1.7$ eV. The dephasing is seen to cause a broadening of the $\tau(E)$ features, but otherwise the behavior of the incoherent ensemble is in perfect accord with that of the coherent packet moving in the absorbing medium. That such two very different systems agree to within fine details suggests that this advancement phenomenon is robust, and it should be expected to occur in real solids.

CONCLUSIONS

The present calculation has revealed a peculiar dynamics of photoelectrons excited by an ultra-short pulse. The interesting features arise from the interplay between the elastic scattering from the crystal lattice and inelastic scattering that causes the damping of the electron wave. Three aspects can be distinguished: first, the effect of inelastic scattering is to increase the average velocity of the wave packet, which is natural because it is the slower components that are damped stronger, as they spend more time in the solid. The range of the advancement effect depends on the interaction with the crystal lattice: at the special points, and around the gaps it may exceed 200 as, whereas in the free-electron-like region it reduces to 20 as, which is still comparable with the measured relative delays, see Fig. 1(b). This effect can be understood in terms of the group velocity of Bloch electrons.

At certain photon energies, however, owing to a complicated non-free-electron-like structure of the final states, the wave packet performs a complicated motion, and it may approach the surface much faster than an instantaneously created packet. This may also lead to an interesting effect that the electron starting from the outermost layer is overtaken by the electron coming from the depth of the crystal.

Close to the spectral gaps the temporal shift of the spectrogram does not necessarily agree with the equation of motion of the center of gravity of the wave packet, but apart from the special points discussed above the discrepancy of the two methods does not exceed 20 as.

This work was supported by the Spanish Ministry of Economy and Competitiveness MINECO (Project No. FIS2013-48286-C2-1-P).

[1] J. C. Slater, Phys. Rev. **51**, 840 (1937).

- [2] V. N. Strocov, R. Claessen, G. Nicolay, S. Hüfner, A. Kimura, A. Harasawa, S. Shin, A. Kakizaki, H. I. Starnberg, P. O. Nilsson, et al., *Phys. Rev. B* **63**, 205108 (2001).
- [3] N. Barrett, E. E. Krasovskii, J.-M. Themlin, and V. N. Strocov, *Phys. Rev. B* **71**, 035427 (2005).
- [4] V. N. Strocov, E. E. Krasovskii, W. Schattke, N. Barrett, H. Berger, D. Schrupp, and R. Claessen, *Phys. Rev. B* **74**, 195125 (2006).
- [5] E. E. Krasovskii, K. Rossnagel, A. Fedorov, W. Schattke, and L. Kipp, *Phys. Rev. Lett.* **98**, 217604 (2007).
- [6] E. E. Krasovskii, W. Schattke, P. Jiříček, M. Vondráek, O. V. Krasovska, V. N. Antonov, A. P. Shpak, and I. Bartoš, *Phys. Rev. B* **78**, 165406 (2008).
- [7] E. E. Krasovskii, J. Höcker, J. Falta, and J. I. Flege, *Journal of Physics: Condensed Matter* **27**, 035501 (2015).
- [8] F. Krausz and M. Ivanov, *Rev. Mod. Phys.* **81**, 163 (2009).
- [9] M. Hentschel, R. Kienberger, C. Spielmann, G. A. Reider, N. Milosevic, T. Brabec, P. Corkum, U. Heinzmann, M. Drescher, and F. Krausz, *Nature* **414**, 509 (2001).
- [10] M. Drescher, M. Hentschel, R. Kienberger, G. Tempea, C. Spielmann, G. A. Reider, P. B. Corkum, and F. Krausz, *Science* **291**, 1923 (2001).
- [11] R. Kienberger, E. Goulielmakis, M. Uiberacker, A. Baltuska, V. Yakovlev, F. Bammer, A. Scrinzi, T. Westerwalbesloh, U. Kleineberg, U. Heinzmann, et al., *Nature* **427**, 817 (2004).
- [12] A. L. Cavalieri, N. Muller, T. Uphues, V. S. Yakovlev, A. Baltuska, B. Horvath, B. Schmidt, L. Blumel, R. Holzwarth, S. Hendel, et al., *Nature* **449**, 1029 (2007).
- [13] J. C. Baggese and L. B. Madsen, *Phys. Rev. A* **78**, 032903 (2008).
- [14] A. K. Kazansky and P. M. Echenique, *Phys. Rev. Lett.* **102**, 177401 (2009).
- [15] C.-H. Zhang and U. Thumm, *Phys. Rev. Lett.* **102**, 123601 (2009).
- [16] A. G. Borisov, D. Sánchez-Portal, A. K. Kazansky, and P. M. Echenique, *Phys. Rev. B* **87**, 121110 (2013).
- [17] C. Lemell, B. Solleder, K. Tórkési, and J. Burgdörfer, *Phys. Rev. A* **79**, 062901 (2009).
- [18] E. E. Krasovskii, V. M. Silkin, V. U. Nazarov, P. M. Echenique, and E. V. Chulkov, *Phys. Rev. B* **82**, 125102 (2010).
- [19] S. Nepl, PhD Thesis, Technische Universität München (2012).
- [20] E. E. Krasovskii, *Phys. Rev. B* **84**, 195106 (2011).
- [21] E. E. Krasovskii and M. Bonitz, *Phys. Rev. Lett.* **99**, 247601 (2007).
- [22] More details of the methodology can be found in Ref. 21, where the model was applied to a single atom.
- [23] The peak position is extracted by fitting the spectrum with a sum of a Gaussian and a linear function to subtract the background. The background comes not only from the inelastically scattered photoelectrons but also from the random potential acting on the initial state.